Quasiperiodic magnetic flux avalanches in doubly connected superconductors

J. Shvartzberg, A. Shaulov, and Y. Yeshurun
Institute of Superconductivity and Institute of Nanotechnology, Department of Physics, Bar-Ilan University, 5290002 Ramat-Gan, Israel

(Received 1 August 2019; revised manuscript received 7 October 2019; published 6 November 2019)

Magneto-optical imaging of Nb rings, open rings, and strips reveals that the topology affects the dendritic flux avalanches in the samples. In particular, dendrites crossing the entire width of the sample appear only in the rings. Such dendrites appear when the difference between the applied field and the average field inside the central hole reaches a certain threshold level $\Delta H_{\rm th}$. With increasing applied field, this condition is reached quasiperiodically as a crossing dendrite creates momentarily a hot channel through which flux flows into the central hole, balancing the field inside the hole with that outside the ring. The threshold $\Delta H_{\rm th}$ differs in magnitude from the onset field $H_{\rm th}$ of magnetic instability, and exhibits qualitatively different dependence on the rim width.

DOI: 10.1103/PhysRevB.100.184506

I. INTRODUCTION

Magneto-optical (MO) imaging has been established as a powerful tool for studying magnetic flux distributions in superconductors. In particular, this technique has been extensively utilized in the study of flux penetration in the form of dendritic avalanches in a variety of superconducting films; for recent works see, e.g., Refs. [1–13]. Magnetic avalanches occur when thermal fluctuations locally release some vortices out of their pinning sites, causing them to move and locally heat the superconductor, thus reducing further the pinning and promoting motion of more vortices. If the heat generated in the film is not dissipated quickly enough, a thermomagnetic runaway occurs, resulting in a dendritic flux avalanche [14,15]. The local temperature rise in the propagation path of the dendrites can reach a high level, well above the critical temperature T_c, [16] and may even exceed the melting temperature of the material [12].

Magneto-optical studies of dendritic avalanches have been mostly carried out on simply connected samples in the form of plates, disks, and strips. It was found that with increasing field above a certain threshold $H_{\rm th}(T)$, dendrites penetrate the samples at random fields and propagate along paths that terminate inside the sample (see, e.g., Ref. [17]). The few MO experiments conducted on multiply connected films in the form of rings [16,18,19] have revealed additional features of the dendritic instability. For example, propagation of flux dendrites of opposite polarities was observed in MgB_2 rings [18]. Also, avalanches injecting flux into the central hole of superconducting MgB_2 rings were observed and exploited to estimate the maximum temperature of the hot channel formed by the dendrites crossing the ring [16].

In this paper, we focus on the distinctive phenomenon observed in superconducting rings, namely, the appearance of a subgroup of dendrites that cross the entire width of the ring, connecting its inner and outer edges. We describe MO results obtained in Nb rings showing that with increasing applied field, crossing dendrites appear quasiperiodically when the difference between the applied field H_a and the field H_i inside the central hole reaches a certain threshold level $\Delta H_{\rm th}$. We find that $\Delta H_{\rm th}$ differs significantly from $H_{\rm th}$. In particular, our measurements of rings of the same diameter but different rim width w show that while $\Delta H_{\rm th}$ increases with w, $H_{\rm th}$ is independent of w. This is in contrast with strips and open rings which exhibit a pronounced decrease of $H_{\rm th}$ with w.

II. EXPERIMENT

A 200-nm-thick Nb film was evaporated on 800-nm SiO_2 substrate. Four sets of samples were patterned on this film, using photolithography followed by reactive ion etching. Each set included a ring, an open ring, and a strip. The open ring has an open channel of width 50 μm extending from the outer to the inner edge. In all sets, the outer diameters of the ring and the open ring were 800 μm. In sets 1, 2, 3, and 4, the width of the strip and the rim of the rings were equal to 50, 100, 200, and 300 μm, respectively.

The MO images were carried out using a custom-made system capable of taking real-time images at rates up to 70 000 frames per second [20]. In the experiments described below, the sample was zero-field cooled to the measurement temperature and the external field, provided by a copper coil, was ramped at a rate of 16.7 Oe/s up to a maximum field of ∼250 Oe. Images were usually taken at a rate of 100 Hz; images at higher rates were taken in an effort to estimate the timescale for the process of crossing vortices reported below.

III. RESULT

The distinctive behavior of dendrites in a ring is demonstrated in Fig. 1 which shows magneto-optical images at $T = 4.5$ K for set 4. Similar images were obtained for the other sets. Note that short-range dendrites (marked in green color in Fig. 1) appear in all three samples; however, a long-range dendrite crossing the entire width of the sample from edge to edge (marked in red color) appears only in the ring. For clarity, we show in Fig. 1(a) only the first crossing dendrite and several short-range dendrites that appear up to a field of 56.7 Oe. For observation of additional short-range and crossing dendrites that appear with increasing field, we refer

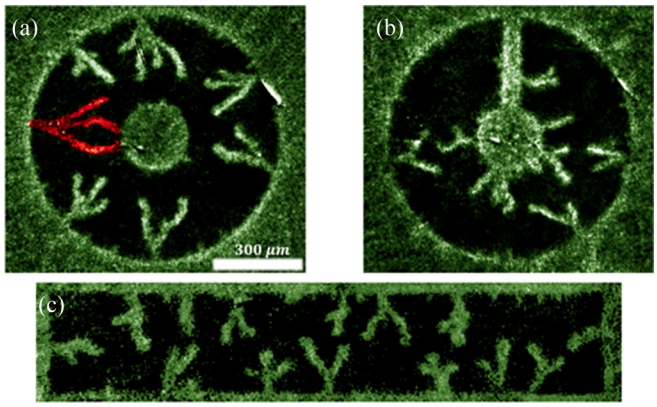

FIG. 1. Magneto-optical images at $T = 4.5$ K of ring (a), open ring (b), and strip (c) in external fields of 56.7, 56.7, and 61.2 Oe, respectively. A long-range dendrite crossing the entire width from edge to edge (marked with red color) appears only in the ring.

the reader to the video in Ref. [21]. Remarkably, in the measured rings of all sets and at all temperatures, the first nucleating dendrite always crosses the entire width of the ring. The appearance of this dendrite is accompanied by a jump of the average field H_i, in the hole, to the value of the applied field H_a, as demonstrated in Fig. 2. With further increasing the applied field, the average field H_i remains essentially constant while several short-range dendrites appear, followed by the next crossing dendrite which balances again the field in the central hole with the applied field. This process gives rise to a stepwise increase in the average field in the hole as illustrated in Fig. 2. The dashed line in the figure describes the line $H_i = H_a$; the jumps of H_i to H_a demonstrate the balance of the field inside the hole and outside the ring, after each crossing dendrite. The quasiperiodic appearance of the crossing dendrites is illustrated in Fig. 3 which shows the difference $\Delta H = H_a - H_i$ as a function of H_a. In each cycle, ΔH increases linearly with H_a and sharply drops to zero when ΔH reaches a certain threshold field, $\Delta H_{\rm th}$, that allows a crossing dendrite. Excluding the first cycle (for a reason

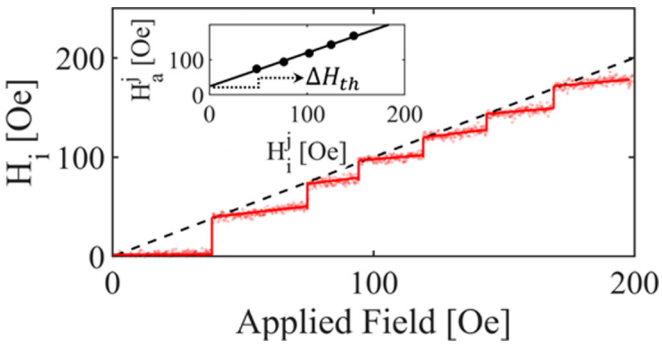

FIG. 2. The average field in the central hole of a ring from set 3 as a function of the external field at $T = 5$ K. The solid red line is a guide to the eye. The stepwise increase in the field occurs when a dendrite crosses the entire rim of the ring. The dashed line describes the line $H_i = H_a$. Inset: The applied field H_a^j versus the average field inside the hole H_i^j, both measured at the onset of the jumps. The solid line is a linear fit of the data to $H_a^j = H_i^j + \Delta H_{\rm th}$.

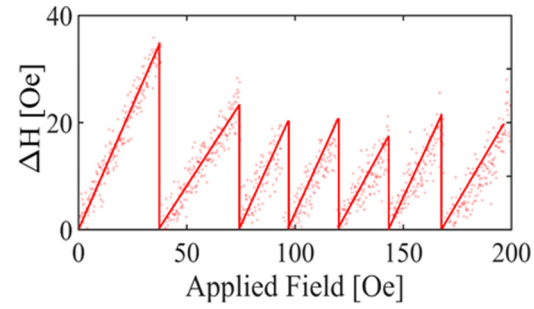

FIG. 3. The difference ΔH between the applied field H_a and the average field inside the hole H_i as a function of H_a at $T = 5$ K, for the same ring as in Fig. 2. In each cycle ΔH increases linearly to $\Delta H_{\rm th}$ and then sharply drops to zero following the appearance of a crossing dendrite. The solid line is a guide to the eye.

to be justified below) the average value of $\Delta H_{\rm th}$ determined from Fig. 3 is 21 Oe. A better estimate of $\Delta H_{\rm th}$ is obtained from a plot (inset of Fig. 2) of the applied field H_a^j, versus the average field inside the hole, H_i^j, both measured at the onset of the jumps shown in Fig. 2. A linear fit of these data (solid line in the inset) yields a slope of 0.96 ± 0.15, reflecting a relationship $H_a^j = H_i^j + \Delta H_{\rm th}$, where $\Delta H_{\rm th} = 24 \pm 5$ Oe is the crossing of this line with the ordinate.

Exclusion of the first jump from the fit is justified because a certain threshold field, $H_{\rm th}$, must be reached for the onset of thermomagnetic instability. In principle, $H_{\rm th}$ may be smaller or larger than $\Delta H_{\rm th}$. In the first case, short-range dendrites precede the appearance of a crossing dendrite, whereas in the second case a crossing dendrite appears first. In fact, in our rings crossing dendrites are always the first to be observed, implying that the first jump in H_i occurs when $H_a = H_{\rm th} > \Delta H_{\rm th}$ and, therefore, it is excluded from the fit which determines $\Delta H_{\rm th}$.

The dependences of $H_{\rm th}$ and $\Delta H_{\rm th}$ on temperature and rim width differ significantly, as demonstrated in Figs. 4 and 5, respectively. Figure 4 shows that $\Delta H_{\rm th}$ is significantly lower

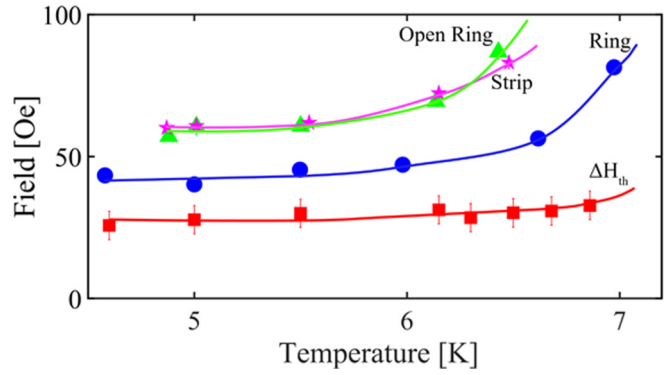

FIG. 4. Temperature dependence of the threshold fields for a ring (circles), an open ring (triangles), and a strip (stars) of the same width from set 3. Also shown is the threshold field $\Delta H_{\rm th}$ (squares) for the appearance of a crossing dendrite in the same ring. The solid lines are a guide to the eye. The error bars for the data points of $H_{\rm th}$ are ~5 Oe. In the $\Delta H_{\rm th}$ data, the error bars are derived from the linear fit of the data to $H_a^j = H_i^j + \Delta H_{\rm th}$.

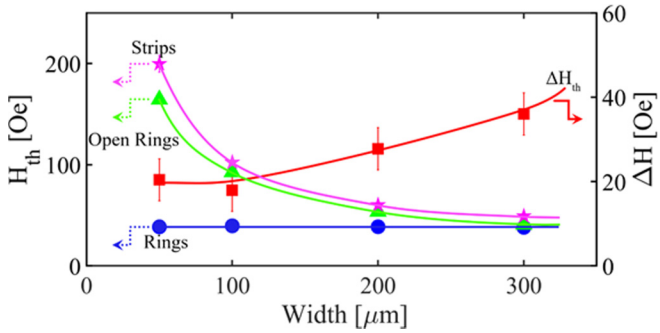

FIG. 5. Width dependence of the threshold field for rings (circles), open rings (triangles), and strips (stars), and $\Delta H_{\rm th}$ (squares) at $T = 5$ K. The solid lines are a guide to the eye. The error bars for the data points of $H_{\rm th}$ are ~5 Oe. In the $\Delta H_{\rm th}$ data, the error bars are derived from the linear fit of the data to $H_a^j = H_i^j + \Delta H_{\rm th}$.

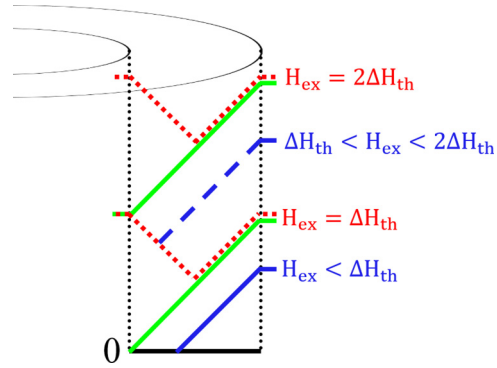

FIG. 6. Schematic illustration of the mechanism for $\Delta H_{\rm th}$. The green solid lines and the red dotted lines describe the induction just before and immediately after the appearance of a crossing dendrite, respectively.

than $H_{\rm th}$ over the entire temperature range. In addition, $\Delta H_{\rm th}$ shows only a moderate increase with temperature as compared to $H_{\rm th}$. A more dramatic, qualitative difference between $\Delta H_{\rm th}$ and $H_{\rm th}$ is demonstrated in their dependence on the rim width. As Fig. 5 shows, $H_{\rm th}$ for rings with the same diameter is independent of the rim width, whereas $\Delta H_{\rm th}$ increases with the width.

For comparison, we also included in Figs. 4 and 5 data for strips and open rings. As shown in Fig. 4, $H_{\rm th}$ for a strip and an open ring are approximately equal and significantly larger than that of the ring. Figure 5 shows that while the threshold field for a ring is independent of the rim width, it decreases strongly with the width for strips and open rings.

IV. DISCUSSION

Our measurements in rings, open rings, and strips demonstrate that the topology of the superconducting sample affects the behavior of dendritic avalanches. In particular, dendrites crossing the entire width of the sample, from edge to edge, appear only in rings (see Fig. 1). Experimentally, we find that the condition for the appearance of a crossing dendrite is that the difference $\Delta H = H_a - H_i$ between the applied field H_a and the average field inside the ring H_i exceeds a certain threshold, $\Delta H_{\rm th}$ (see Figs. 2 and 3). With increasing the applied field, this condition is reached quasiperiodically as a crossing dendrite resets the system by creating, for a short time, a hot channel through which flux flows into the central hole, balancing the field inside and outside the ring [16]. As a result, a staircase increase in the average flux inside the central hole of the ring is obtained.

The mechanism for a periodic $\Delta H_{\rm th}$ can be easily grasped considering a simplified model in which the crossing dendrite propagates on a background [15] of a Bean-like induction profile, as described in Fig. 6. Initially, after zero-field cooling, the field inside the hole is zero and the field penetrates the ring only from outside (solid blue line), consequently, the slope of the induction in the ring does not change sign. As the external field is increased to the level of $\Delta H_{\rm th}$ (assuming for simplicity that $\Delta H_{\rm th} > H_{\rm th}$), (solid green line in Fig. 6), a propagating dendrite faces no resistance from the background induction field and it crosses the entire ring, balancing the external field with the field inside the hole. The external field and the field inside the hole result in field penetration from both sides of the rim (dotted red line in the figure). In this situation, the propagation of the next dendrite is impeded by an opposite Lorentz force [22] created by the opposite induction slope. Upon increasing the external field, the field inside the hole remains trapped and, therefore, an imbalance between the external field and the field in the hole is created (blue dashed line in the figure). The opposite force experienced by the propagating dendrite diminishes as the external field is increased to $2\Delta H_{\rm th}$ (red dotted line) preparing the ground for the next crossing dendrite. This process repeats itself as the external field increases to $3\Delta H_{\rm th}$, etc. This simplified model implies an increase of $\Delta H_{\rm th}$ with the rim width w : $\Delta H_{\rm th} = \mu_0 J w$, where J is the slope of the induction profile. Clearly, this model should be refined considering the actual induction profiles of a ring in a perpendicular field and the effect of trapped dendrites on these profiles. Nevertheless, it captures the essence of the experimentally observed threshold field $\Delta H_{\rm th}$ and the quasiperiodic appearance of the crossing dendrites at field intervals of $\Delta H_{\rm th}$. In contrast to a ring, in a simply connected sample, such as a strip, the field penetration from opposite sides of the sample is symmetric. Thus, a dendrite emerging from one side experiences a Lorentz force driving it into the sample center [22] and then it experiences an opposite force exerted by the *same* current flowing in the opposite direction. This explains why in such samples, propagating dendrites terminate inside the sample.

The origin of the different behavior of dendrites in a ring as compared to simply connected samples can also be explained in the case that the dendrites experience Lorentz force due to Meissner screening currents only. The screening current in simply connected samples flows uniformly along the sample edge, whereas in a ring the screening current along the outer edge is usually larger than that flowing in the inner edge [18,23,24]. A dendrite emerging from the edge in a simply connected sample, such as a strip, experiences a Lorentz force driving it into the sample center [22] and then it experiences an opposite force exerted by the *same* current flowing in the opposite direction. Consequently, the propagating dendrites terminate inside the sample. In a ring, however, the difference

between the currents flowing in the outer and inner edges can drive dendrites across the entire rim width provided that this difference exceeds a certain threshold $\Delta I_{\rm th}$. Obviously, the condition $\Delta I = \Delta I_{\rm th}$ cannot be fulfilled in simply connected samples, as the screening current flows continuously along the sample edge, implying $\Delta I \equiv 0$. Experimentally, the difference ΔI is borne out as a difference ΔH between the applied field and the field inside the hole. This is obviously true in the hypothetical case of a long, hollow cylinder in which ΔH is directly generated by ΔI. In this hypothetical case, the appearance of a crossing dendrite would be periodic with the applied field with an exact periodicity of $\Delta H_{\rm th}$. This is because after each crossing dendrite, the injected flux inside the hole remains trapped and constant, until the increasing applied field exceeds again by $\Delta H_{\rm th}$, balancing again the field inside the hole and outside the cylinder. In the realistic case of a flat ring, $\Delta H_{\rm th}$ is still related to $\Delta I_{\rm th}$ but the periodicity is somewhat disrupted because the field in the central hole varies slightly due to demagnetization effects that cause flux leakage into the hole. As a result, although the appearance of crossing dendrites is periodic with $\Delta H = H_a - H_i$, it is only quasiperiodic with the applied magnetic field H_a.

The "inversion scheme" described by Wijngaarden *et al.* [25] (see also Brandt, Ref. [26]) and the MATLAB code provided by Qviller [27], allow demonstrating the effect of crossing dendrites on the current distribution in a ring. Maps of current distributions in a ring in different fields are shown in Fig. 7. For comparison we also show in Fig. 7(a) a map of the current density distribution in an open ring exhibiting a uniform current along its edge. Figures 7(b) and 7(c), respectively, illustrate the current distribution in the ring before the appearance of the first crossing dendrite ($H_a = 34.6$ Oe) and immediately after the crossing ($H_a = 36$ Oe). Apparently, before the crossing, the current along the outer edge exceeds that of the inner edge, and those become equal after the crossing. Note that the current pattern after the crossing is similar to that observed in the open ring. This similarity reflects the imprint of the flux frozen in the hot channel created by the crossing dendrite. Upon increasing the field to 53.3 Oe, just before the entry of the second crossing dendrite, the difference between the current flowing in the outer and inner edges is reestablished, as demonstrated in Fig. 7(d). At 58 Oe, just after the crossing of the second dendrite, a current distribution with an imprint of the second channel is observed, see Fig. 7(e).

As mentioned above, the condition $\Delta H = \Delta H_{\rm th}$ for a crossing dendrite in a ring differs from the condition $H_a = H_{\rm th}$ for the appearance of the first dendrite which may or may not cross the rim. Measurements in our Nb rings show that $H_{\rm th} > \Delta H_{\rm th}$, see Figs. 4 and 5, and therefore, the *first* observed dendrite in these rings always crossed the rim. These figures also show that the temperature and the width dependence of $\Delta H_{\rm th}$ differ from that of $H_{\rm th}$. Specifically, $H_{\rm th}$ increases strongly with temperature, consistent with previous reports [28,29], whereas $\Delta H_{\rm th}$ is almost temperature independent. This behavior of $\Delta H_{\rm th}$ can be ascribed to a decrease of the critical current with temperature, resulting in a competition between two mechanisms: On the one hand the decrease of the critical current makes the sample more susceptible to smooth flux entry [28], and, consequently, requires higher $\Delta H_{\rm th}$ to drive a dendrite across the entire width of the rim. On the other hand, a decrease of $\Delta H_{\rm th}$ is expected with decreasing of the current, as apparent from Fig. 6.

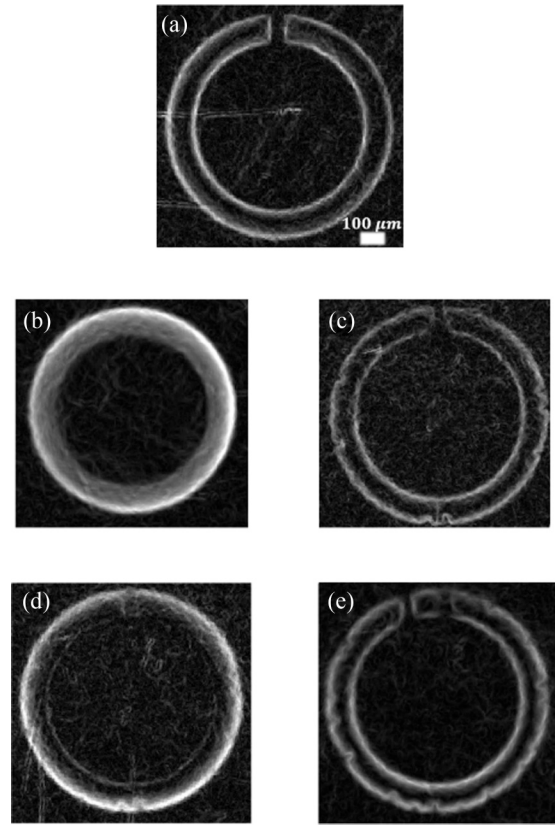

FIG. 7. Maps of current distribution at $T = 4.8$ K in an open ring (a) from set 2 in an external field of 36 Oe and in a ring from the same set in external fields of 34.6 Oe [(b) just before the appearance of the first crossing dendrite], 36 Oe [(c) immediately after the crossing], 53.3 Oe [(d) just before the appearance of the second crossing dendrite], and 58 Oe [(e) immediately after the second crossing].

An additional difference between $H_{\rm th}$ and $\Delta H_{\rm th}$ is manifested in their dependence on the width of the rim; see Fig. 5. While $H_{\rm th}$ is independent of the rim width w, $\Delta H_{\rm th}$ increases with w. To explain the independence of $H_{\rm th}$ on w we note that the measured threshold field for the entry of the first dendrite depends on the demagnetization factor D of the sample. As for a ring (and for a disk) D depends only on the ratio of the film thickness to the diameter [23,24,30], and since all the rings in our experiment are made of the same film (200 nm thick) and they have the same diameter (800 μm), the threshold field is expected to be independent of the rim width. Indeed, our measurements show that the threshold field for all the rings coincides with that of a disk of the same thickness and same diameter at all temperatures.

In Fig. 5 we also show the width dependence of the threshold field of the strips at $T = 5$ K. The decrease of this threshold field with the width is consistent with that reported by Johansen *et al.* for MgB_2 [29] strips. Nevertheless, an alternative explanation to the observed decrease can be based on the increase of the demagnetization factor as the width of the strip increases. In fact, the factor of 4 difference between

the value of the threshold fields of a ring and a strip of the same width can also be ascribed to the difference between their demagnetization factors, the latter being much larger for a ring.

Finally, we note that the limitations imposed by thermomagnetic avalanches on potential applications of superconductors become more severe in using multiply connected structures such as rings. A crossing dendrite in rings may cause a sudden change in the magnetic field in the area enclosed by the ring, leading to the generation of large electromotive force. Our experiment in Nb rings shows that the step increase in the average field inside the hole, see Fig. 2, is extremely sharp and it could not be resolved even by using a high imaging rate of 21 kHz. This indicates a lower bound of 80 T/s for the rate of change of the field inside the hole. If such a ring is used for screening a sensitive electronic device from external fields, the generated large electromotive force may damage the device.

V. SUMMARY AND CONCLUSIONS

Our magneto-optical studies show that the topology, as well as the geometry, of superconducting samples affect the behavior of dendritic flux avalanches in the sample. We identify two subgroups of dendrites, those that terminate inside the sample and those that cross the entire width of the sample. While in simply connected samples only dendrites of the first group are observed, in multiply connected samples, such as rings, both groups exist. A necessary condition for the appearance of dendrites of both kinds is that the external field exceeds a certain threshold. However, an additional condition is required for the appearance of a dendrite crossing from edge to edge, namely, that the difference between the external field and the field inside the hole exceeds a certain threshold $\Delta H_{\rm th}$. As the external field increases, this threshold is reached quasiperiodically. The crossing dendrites impose additional limitations on potential use of thin superconducting layers in practical applications.

ACKNOWLEDGMENTS

We thank Michael Stern for providing the Nb films. Thanks are also extended to Michael Baziljevich, Elran Baruch-El, Boris Shapiro, and Leonid Burlachkov for helpful discussions. We acknowledge the help provided by Atle Jorstad Qviller with the inversion scheme from the Github repository.

[1] E. Polturak, J. Low Temp. Phys. **197**, 310 (2019).
[2] F. Colauto, D. d. Carmo, A. M. H. d. Andrade, A. A. M. Oliveira, W. A. Ortiz, Y. M. Galperin, and T. H. Johansen, IEEE Trans. Appl. Supercond. **29**, 1 (2019).
[3] S. Blanco Alvarez, J. Brisbois, S. Melinte, R. B. G. Kramer, and A. V. Silhanek, Sci. Rep. **9**, 3659 (2019).
[4] T. Qureishy, J. I. Vestgården, A. J. Qviller, A. S. Fjellvåg, J. M. Meckbach, A. Torgovkin, T. H. Johansen, K. Ilin, M. Siegel, I. Maasilta, and P. Mikheenko, AIP Adv. **8**, 085128 (2018).
[5] E. Baruch-El, M. Baziljevich, T. H. Johansen, X. Y. Zhou, X. Q. Jia, B. B. Jin, A. Shaulov, and Y. Yeshurun, Supercond. Sci. Technol. **31**, 105008 (2018).
[6] V. K. Vlasko-Vlasov, F. Colauto, A. I. Buzdin, D. Rosenmann, T. Benseman, and W. K. Kwok, Phys. Rev. B **95**, 174514 (2017).
[7] V. K. Vlasko-Vlasov, F. Colauto, A. I. Buzdin, D. Rosenmann, T. Benseman, and W. K. Kwok, Phys. Rev. B **95**, 144504 (2017).
[8] T. Qureishy, C. Laliena, E. Martínez, A. J. Qviller, J. I. Vestgården, T. H. Johansen, R. Navarro, and P. Mikheenko, Supercond. Sci. Technol. **30**, 125005 (2017).
[9] J. Brisbois, V. N. Gladilin, J. Tempere, J. T. Devreese, V. V. Moshchalkov, F. Colauto, M. Motta, T. H. Johansen, J. Fritzsche, O. A. Adami, N. D. Nguyen, W. A. Ortiz, R. B. G. Kramer, and A. V. Silhanek, Phys. Rev. B **95**, 094506 (2017).
[10] C. Di Giorgio, F. Bobba, A. M. Cucolo, A. Scarfato, S. A. Moore, G. Karapetrov, D. D'Agostino, V. Novosad, V. Yefremenko, and M. Iavarone, Sci. Rep. **6**, 38557 (2016).
[11] J. Brisbois, M. Motta, J. I. Avila, G. Shaw, T. Devillers, N. M. Dempsey, S. K. P. Veerapandian, P. Colson, B. Vanderheyden, P. Vanderbemden, W. A. Ortiz, N. D. Nguyen, R. B. G. Kramer, and A. V. Silhanek, Sci. Rep. **6**, 27159 (2016).
[12] M. Baziljevich, E. Baruch-El, T. H. Johansen, and Y. Yeshurun, Appl. Phys. Lett. **105**, 012602 (2014).
[13] J. I. Vestgården, D. V. Shantsev, Y. M. Galperin, and T. H. Johansen, Sci. Rep. **2**, 886 (2012).
[14] I. S. Aranson, A. Gurevich, M. S. Welling, R. J. Wijngaarden, V. K. Vlasko-Vlasov, V. M. Vinokur, and U. Welp, Phys. Rev. Lett. **94**, 037002 (2005).
[15] D. V. Denisov, A. L. Rakhmanov, D. V. Shantsev, Y. M. Galperin, and T. H. Johansen, Phys. Rev. B **73**, 014512 (2006).
[16] A. A. F. Olsen, T. H. Johansen, D. Shantsev, E.-M. Choi, H.-S. Lee, H. J. Kim, and S.-l. Lee, Phys. Rev. B **76**, 024510 (2007).
[17] T. H. Johansen, M. Baziljevich, D. V. Shantsev, P. E. Goa, Y. M. Galperin, W. N. Kang, H. J. Kim, E. M. Choi, M. S. Kim, and S. I. Lee, Supercond. Sci. Technol. **14**, 726 (2001).
[18] A. A. F. Olsen, T. H. Johansen, D. Shantsev, E.-M. Choi, H.-S. Lee, H. J. Kim, and S.-l. Lee, Phys. Rev. B **74**, 064506 (2006).
[19] M. Pannetier, F. C. Klaassen, R. J. Wijngaarden, M. Welling, K. Heeck, J. M. Huijbregtse, B. Dam, and R. Griessen, Phys. Rev. B **64**, 144505 (2001).
[20] M. Baziljevich, D. Barness, M. Sinvani, E. Perel, A. Shaulov, and Y. Yeshurun, Rev. Sci. Instrum. **83**, 083707 (2012).
[21] superconductivity.biu.ac.il/node/1064.
[22] T. H. Johansen, M. Baziljevich, D. V. Shantsev, P. E. Goa, Y. M. Galperin, W. N. Kang, H. J. Kim, E. M. Choi, M. S. Kim, and S. I. Lee, EPL **59**, 599 (2002).
[23] E. H. Brandt, Phys. Rev. B **55**, 14513 (1997).
[24] E. H. Brandt and J. R. Clem, Phys. Rev. B **69**, 184509 (2004).
[25] R. J. Wijngaarden, H. J. W. Spoelder, R. Surdeanu, and R. Griessen, Phys. Rev. B **54**, 6742 (1996).

[26] E. H. Brandt, Phys. Rev. B **46**, 8628 (1992).
[27] A. J. Qviller, arXiv:1903.09130.
[28] E. Baruch-El, M. Baziljevich, B. Y. Shapiro, T. H. Johansen, A. Shaulov, and Y. Yeshurun, Phys. Rev. B **94**, 054509 (2016).
[29] D. V. Denisov, D. V. Shantsev, Y. M. Galperin, E.-M. Choi, H.-S. Lee, S.-I. Lee, A. V. Bobyl, P. E. Goa, A. A. F. Olsen, and T. H. Johansen, Phys. Rev. Lett. **97**, 077002 (2006).
[30] C. Du-Xing, E. Pardo, and A. Sanchez, IEEE Trans. Magn. **38**, 1742 (2002).